

The thermoinsulation effect of snow cover within a climate model

Benjamin I. Cook · Gordon B. Bonan ·
Samuel Levis · Howard E. Epstein

Received: 24 April 2007 / Accepted: 7 November 2007
© Springer-Verlag 2007

Abstract We use a state of the art climate model (CAM3–CLM3) to investigate the sensitivity of surface climate and land surface processes to treatments of snow thermal conductivity. In the first set of experiments, the thermal conductivity of snow at each grid cell is set to that of the underlying soil (SC-SOIL), effectively eliminating any insulation effect. This scenario is compared against a control run (CTRL), where snow thermal conductivity is determined as a prognostic function of snow density. In the second set of experiments, high (SC-HI) and low (SC-LO) thermal conductivity values for snow are prescribed, based on upper and lower observed limits. These two scenarios are used to envelop model sensitivity to the range of realistic observed thermal conductivities. In both sets of experiments, the high conductivity/low insulation cases

show increased heat exchange, with anomalous heat fluxes *from the soil to the atmosphere* during the winter and *from the atmosphere to the soil* during the summer. The increase in surface heat exchange leads to soil cooling of up to 20 K in the winter, anomalies that persist (though damped) into the summer season. The heat exchange also drives an asymmetric seasonal response in near-surface air temperatures, with boreal winter anomalies of +6 K and boreal summer anomalies of −2 K. On an annual basis there is a net loss of heat from the soil and increases in ground ice, leading to reductions in infiltration, evapotranspiration, and photosynthesis. Our results show land surface processes and the surface climate within CAM3–CLM3 are sensitive to the treatment of snow thermal conductivity.

Keywords Snow cover · Snow thermal conductivity · Climate model sensitivity · Soil/atmosphere exchange · Permafrost

B. I. Cook (✉)
Lamont Doherty Earth Observatory, Ocean and Climate Physics,
61 Route 9W, PO Box 1000, Palisades, NY 10964-8000, USA
e-mail: bc9z@ldeo.columbia.edu

B. I. Cook
NASA Goddard Institute for Space Studies,
2880 Broadway, New York, NY 10025, USA

G. B. Bonan
National Center for Atmospheric Research,
1850 Table Mesa Drive, Boulder, CO 80307-3000, USA

S. Levis
National Center for Atmospheric Research,
1850 Table Mesa Drive, Boulder, CO 80307-3000, USA

H. E. Epstein
Department of Environmental Sciences, University of Virginia,
291 McCormick Road, Charlottesville, VA 22903, USA

1 Introduction

Snow cover is a major component of the cryosphere and the climate system (e.g. Barnett et al. 1989; Cess et al. 1991; Cohen and Rind 1991; Cohen and Entekhabi 1999). In the Northern Hemisphere, snow covers (on average) ~ 1.9 million km^2 at its minimum extent in August and ~ 45.2 million km^2 at its maximum extent in January (Barry et al. 2007). Snow covers a much more restricted area in the Southern Hemisphere, ~ 14.5 million km^2 (mostly over Antarctica), with limited seasonal melting along the Antarctic peninsula and western Antarctic coast. The extent and depth of snow in the Northern Hemisphere displays substantial interannual variability, making it one of the most important seasonally and interannually varying

components of the land surface (Armstrong and Brodzik 2005; Barry et al. 2007; Brown 2000). The vast majority of model studies investigating the role of snow cover in the climate system have focused on the effect of snow on the land surface albedo (e.g., Cess et al. 1991; Hall 2004; Hall and Qu 2006; Qu and Hall 2006; Randall et al. 1994). Snow, typically, has a higher albedo than either bare ground or vegetation, and the presence of snow can lead to sharp increases in reflected radiation, leading to lower surface temperatures. Through its modulation of surface albedo, snow cover is considered an important feedback within the climate system, especially when amplified by the retreat and advance of boreal vegetation (e.g., Bonan et al. 1992; Gallimore et al. 2005).

Few investigations within the climate modeling community have looked at the role of snow from the perspective of thermal conductivity. Snow has a relatively low thermal conductivity compared to many materials, including mineral soil and organic matter, making it an effective thermal insulator (Goodrich 1982; Sokratov and Barry 2002; Zhang et al. 1996, 1997, 2005). The conductivity changes over time, and typical conductivities range from 0.10 (for fresh or new snow) to 0.50 (for compacted or partially melted snow) $\text{W m}^{-1} \text{K}^{-1}$ (Zhang 2005). The total insulation effect can also be altered by changing snow amount; i.e. snow presence or absence and snow depth (Sokratov and Barry 2002). Snow effectively retards heat exchange between the soil and the overlying atmosphere, allowing soils to maintain temperatures of 10–15 K warmer than the overlying atmosphere during winter (e.g., Molders and Walsh 2004). This insulative effect is greatest during the fall and early winter, when snow is less dense and a more effective insulator; this contrasts with the albedo effect of snow, which is greatest during the spring, when solar insolation rates are higher (Ling and Zhang 2003; Vavrus 2007; Zhang et al. 2001; Zhang 2005).

Through its modulation of soil-atmosphere heat exchange, snow is an important variable for permafrost and active layer modeling (e.g., Shiklomanov and Nelson 1999; Sazonova and Romanovsky 2003). In some cases it may even be the dominant controlling factor on whether permafrost is present or absent (Zhang 2005). By modifying the snow thermal regime, insulation from snow cover can also indirectly affect soil hydrology by affecting the relative proportion of ice versus liquid water content in the soil, altering rates of infiltration, drainage, and runoff (Cary et al. 1978; Luo et al. 2003; Niu and Yang 2006; Willis et al. 1961). Changes in soil temperatures and hydrology can further cascade to influence ecological processes, particularly at high latitudes where there is concern about land surface and carbon cycle feedbacks to climate change. These include changes in soil microbial activity, plant

nutrient availability, and vegetation (Chapin et al. 1995; Sturm et al. 2001, 2005).

Given how important snow is for regulating soil temperatures in certain regions, it is worth considering how sensitive climate models are to the parameterization of snow thermal conductivity, and what this important variable means for the surface climate and land surface processes within these models. We conduct several modeling experiments using the atmosphere and land components from a general circulation model. Our experiments are designed to illuminate how sensitive the climate system and land surface are to treatments of snow thermal conductivity. In the first, purely theoretical case, we set the thermal conductivity of the snow equal to that of the first soil layer below. This experiment essentially removes *any* insulative effect and is designed to explore the full sensitivity of the model climate. The results are compared against a control simulation with prognostic snow thermal conductivity. Second, we set the thermal conductivity of the snow to maximum and minimum values, based on a review of observed values (Zhang 2005). These latter two experiments, therefore, are designed to give insight into how the climate and ground thermal regime may respond within more realistic bounds.

2 Methods

2.1 Model description

We use the atmosphere and land models from the National Center for Atmospheric Research (NCAR) Community Climate System Model version 3 (CCSM3; Collins et al. 2006). CCSM3 shows substantial improvements in the simulations of sea ice, polar radiation budgets, sea surface temperatures, and cloud radiative effects, compared to previous versions of the model. In fully coupled mode, it produces a stable mean climate without flux adjustments.

The atmospheric model we use is the community atmosphere model version 3 (CAM3) (Hurrell et al. 2006). This model is the sixth generation of atmospheric general circulation models developed by the climate community in collaboration with the National Center for Atmospheric Research. The model features improvements to the parameterizations of moist processes, radiation processes, and aerosols (Collins et al. 2004, 2006) compared with its predecessor, CAM2. CAM3 includes more physically realistic treatments of cloud and precipitation processes, including explicit computation of snow (Boville et al. 2006). The model shows improved simulations of precipitation over the previous version, although the model still overestimates precipitation poleward of the extratropical storm tracks (Hack et al. 2006). The model was run using

Eulerian spectral dynamics with T42 spectral truncation (approximately 2.8° in latitude and longitude) with 26 levels in the vertical and a 20-min time step. The land model is the community land model version 3 (CLM3), operating on the same spatial grid as CAM3. CLM3 simulates energy, moisture, and momentum fluxes between the land and atmosphere, the hydrologic cycle at the land surface, and soil temperature (Bonan et al. 2002; Oleson et al. 2004; Dickinson et al. 2006). There is a warm bias for the cold season in CAM3–CLM3, primarily at high latitudes, due to excessive low clouds produced by CAM3 that increase downward longwave radiation fluxes (Dickinson et al. 2006). This bias leads to higher than observed winter precipitation and higher than observed snow depths. Additionally, the snow model does not account for sublimation from blowing snow, a process that can lead to significant losses of snow mass (Hinzman et al. 1996; Kane et al. 1991; Serreze et al. 2003). Neglecting this process leads to simulated snow packs that are deeper than observed and subsequent spring runoff that is too high. Due to an oversight, CLM3 does not allow for snow aging except in snow deep enough to have five layers (deeper than about 0.5 m). Fully implemented snow aging would have lowered the albedo for older snow, although CLM3 already underestimates springtime albedo in snow-covered areas relative to satellite estimates (Lawrence and Chase 2007). The version of CLM3 used in these experiments includes substantial improvements to the land surface hydrology (Lawrence et al. 2007). These improvements help reduce a dry soil bias in the standard version CLM3, leading to better simulations of photosynthesis and vegetation dynamics, increased transpiration and infiltration of water into the soil, and improved partitioning of evapotranspiration among canopy evaporation, bare soil evaporation, and transpiration. The current version of CLM3 does not include an organic matter layer, has a soil column depth of only 3.43 m, and solves temperature dynamics in a two-step procedure. These factors lead to inaccurate simulations of permafrost and soil temperatures over many areas, compared to observations (Alexeev et al. 2007; Nicolsky et al. 2007). For 20th century climate, however, the model does a reasonable job reproducing the current permafrost distribution (Lawrence and Slater 2005).

Thermal conductivity of the snow in CLM3 is based on Jordan (1991):

$$\lambda_{\text{snow}} = \lambda_{\text{air}} + (7.75 \times 10^{-5} \rho_{\text{snow}} + 1.105 \times 10^{-6} \rho_{\text{snow}}^2) (\lambda_{\text{ice}} - \lambda_{\text{air}}) \quad (1)$$

where λ_{snow} is snow thermal conductivity, λ_{air} is air thermal conductivity, λ_{ice} is ice thermal conductivity, and

ρ_{snow} is the snow density. As snow density increases, either through increasing snow mass or decreasing snow height (compaction), the thermal conductivity increases, reducing the insulative effect. This behavior is designed to mimic what happens in nature, where snow compaction or melting reduces the air content of a given volume of snow, a common result towards the end of the snow season. Within CLM3, compaction occurs as a result of destructive metamorphism (function of temperature), overburden (function of snow load pressure), and melting/refreezing (also a function of temperature) (Oleson et al. 2004). In our control run of CLM, the interquartile range for λ_{snow} is 0.149–0.459 for the Northern Hemisphere and 0.532–0.684 for the Southern Hemisphere. Median λ_{snow} values from our control simulation are shown in Fig. 1. For much of the Northern Hemisphere, a clear seasonality in λ_{snow} is apparent. Values are low in the beginning of the snow season (SON and DJF), and increase towards the end (MAM). Over certain regions, notably Greenland and Antarctica, there is little seasonal change in λ_{snow} . These areas have snow depths of up to 3 m (Fig. 2) and persistent snow cover (Fig. 3) year round. Because the snow persists seasonally and inter-annually, the snow column is dominated by the older, compacted snow, and this is reflected in the higher conductivities. Greenland makes up a relatively small proportion of the snow covered land in the Northern Hemisphere, at least during winter, and has little impact on the total hemispheric distribution of conductivity values. Conversely, Antarctica makes up most of the snow-covered area in the Southern Hemisphere, and the distribution of λ_{snow} values in the Southern Hemisphere largely reflects this. Certain areas (Fig. 1, in red) also show exceptionally high values for λ_{snow} (these values exceed the high end of the color scale, which was scaled back for greater contrast at low values). Around Greenland, these values are in the range of 2–3 $\text{W m}^{-1} \text{K}^{-1}$ over areas with persistently deep snow. These high values also typically appear in warmer seasons or around the margins of the snow-covered area; values can range as high as 5–20 $\text{W m}^{-1} \text{K}^{-1}$. These high thermal conductivities fall well outside the range of typical observed values, but we note that, within the model, the abnormally high values typically occur in areas with very shallow snow depths (Fig. 2) and low fractional snow coverage (Fig. 3). These are situations where the effectiveness of snow as a ground insulator would be small anyway, and it should have little impact on our results. For comparison, we show climatological observations of snow cover in Fig. 4 to compare against our control simulation (Fig. 3). Observations are only available for the Northern Hemisphere. Direct comparison is difficult for a variety of reasons, including different spatial

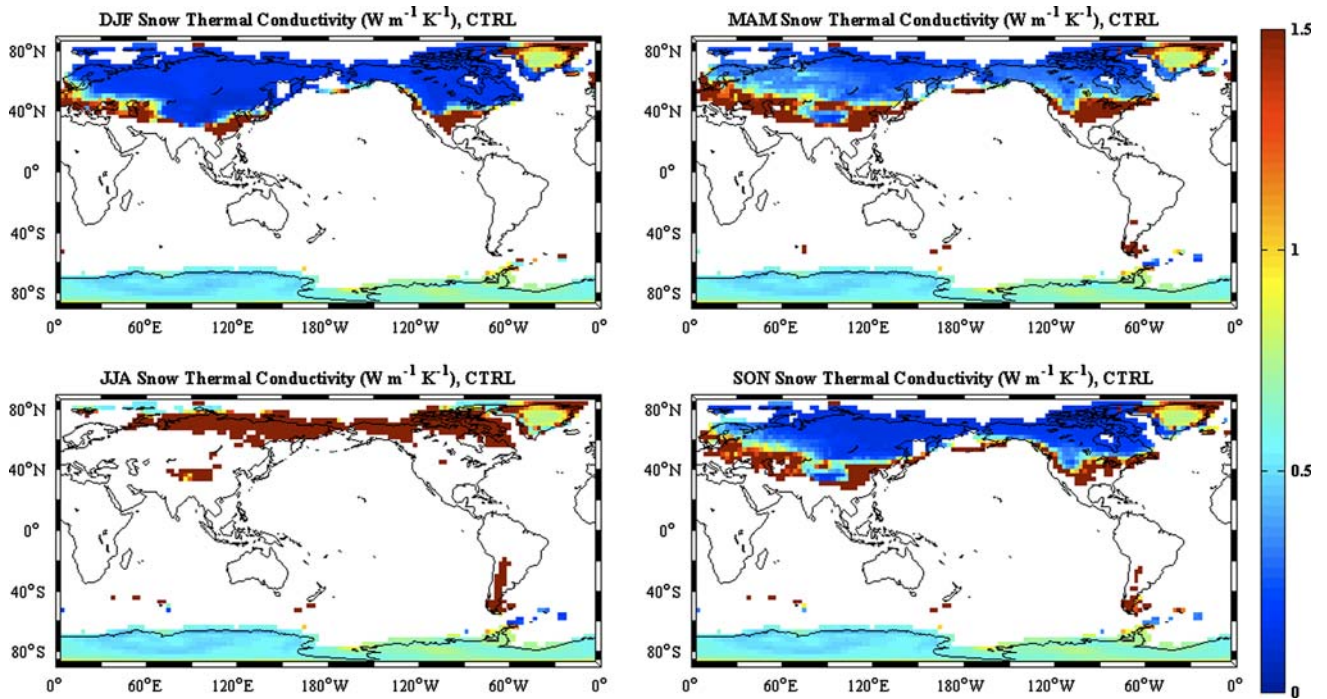


Fig. 1 Seasonal plots of prognostic snow thermal conductivity from thirty years of our control run

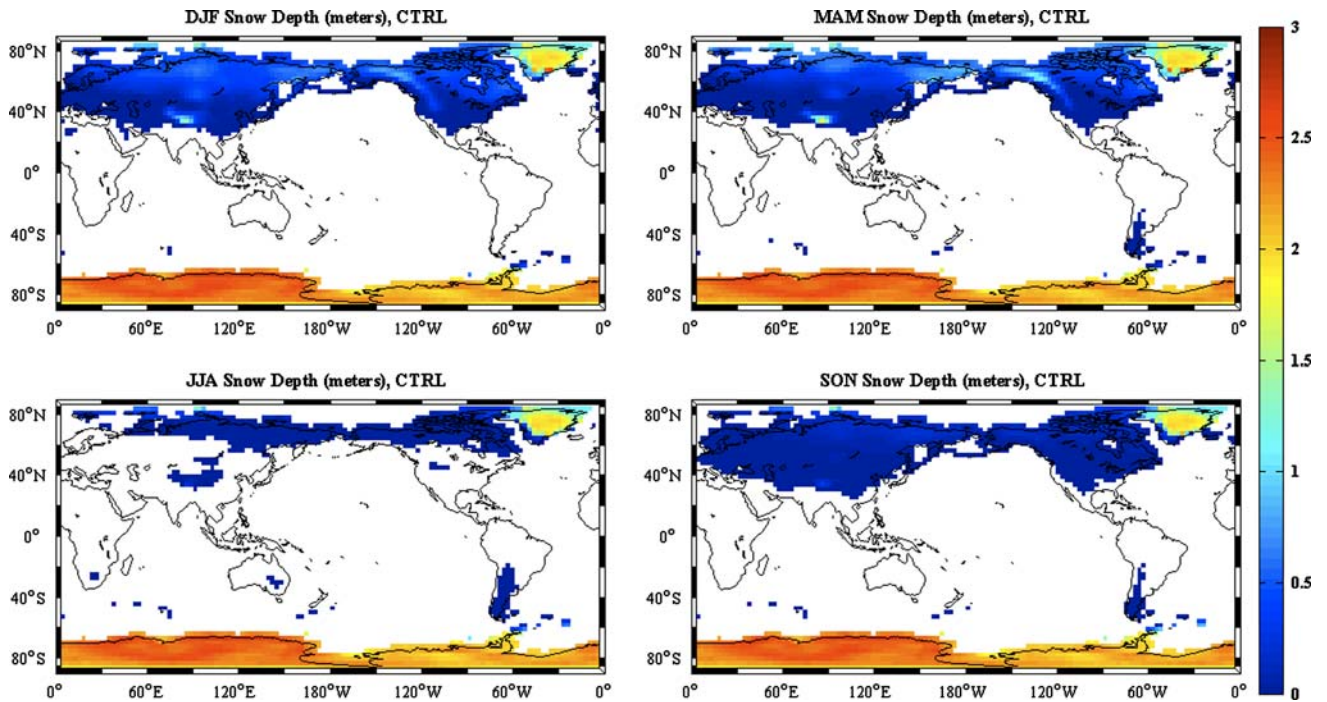


Fig. 2 As Fig. 1, but for snow depth

resolutions and algorithms for determining fractional coverage. The spatial pattern and seasonal cycle of snow cover is reproduced reasonably well by the model,

though there is a tendency to underestimate snow cover fraction through all four seasons. Previous studies have shown that fractional snow coverage in CCSM3 is biased

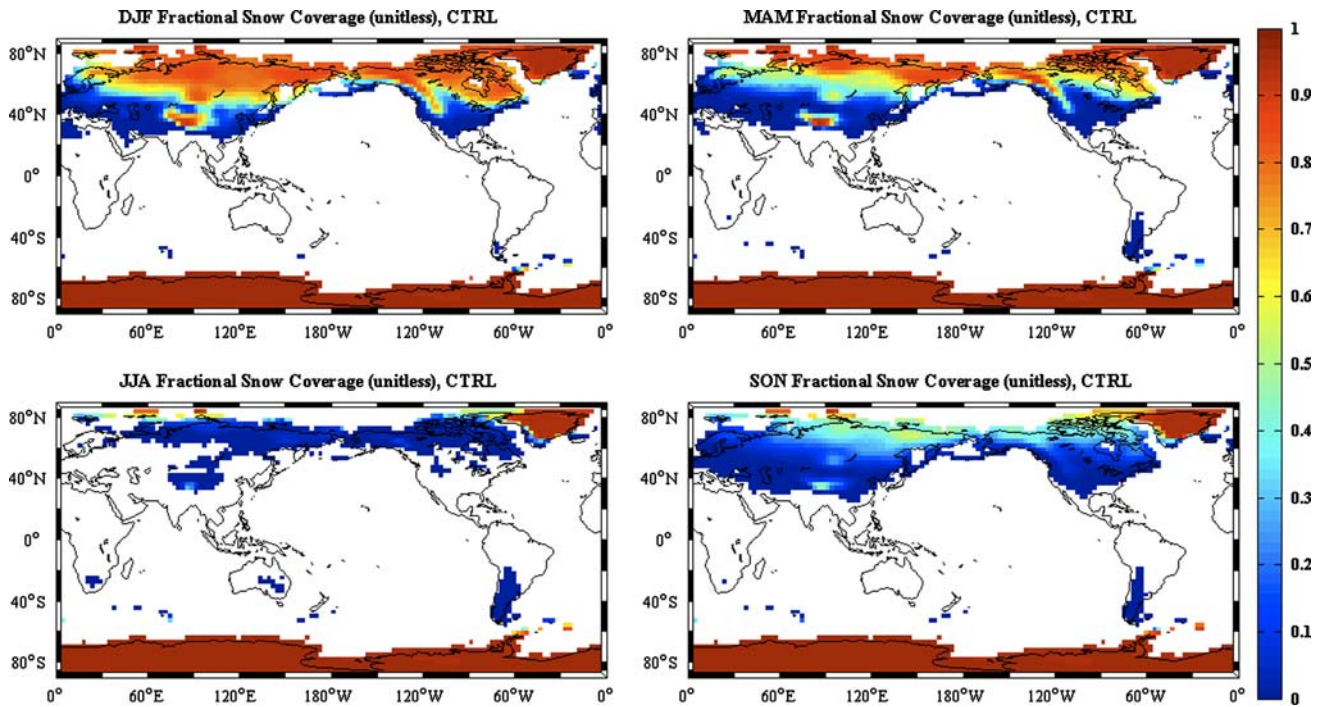


Fig. 3 As Fig. 1, but for snow cover fraction

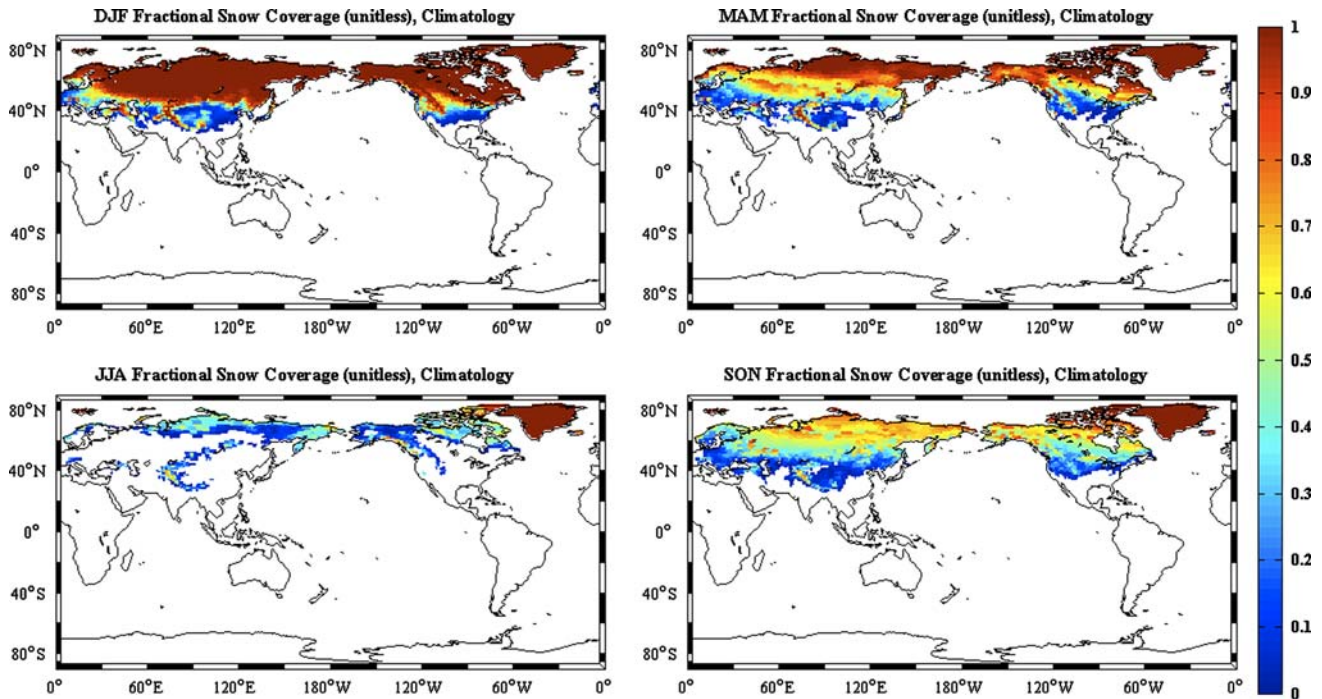


Fig. 4 Seasonal (DJF, MAM, JJA, SON) climatology of observed snow cover fraction (data from <http://climate.rutgers.edu/snowcover/>)

low compared to observations, and is also low compared to other models (Frei and Gong 2005).

The soil thermal conductivity (used in place of the prognostic snow thermal conductivity in experiment SC-

SOIL, described later) is based on Farouki (1981), determined as a function of soil properties (sand/silt/clay content, porosity, bulk density), degree of saturation, liquid water content, and ice content (Oleson et al. 2004). As soil

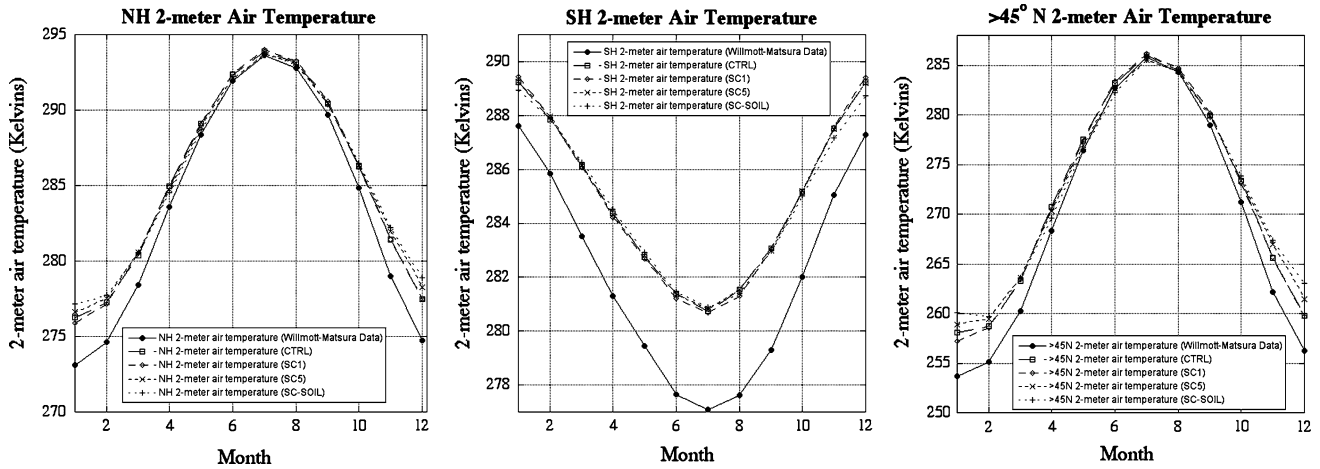


Fig. 5 Seasonal cycles in 2-m air temperatures over land (Kelvins) from the Willmott–Matsura validation dataset and our model simulations (CTRL, SC1, SC5, and SC-SOIL). Shown are the cycles from the Northern Hemisphere, Southern Hemisphere, and land areas north of 45° N

water content (liquid or ice) increases, the conductivity increases as well.

2.2 Experimental setup

Our study looks at climate and land surface responses to snow thermal conductivity values based on both theoretical limits and more realistic values. The theoretical approach (used in so-called ‘maximum effect’ experiments) has been used extensively over the history of climate modeling to examine the maximum sensitivity of climate models to various boundary conditions. Examples include studies where evapotranspiration from the land surface is turned off (Shukla and Mintz 1982), where global vegetation is alternated between desert and forest (Kleidon et al. 2000), and where snow is completely removed from the land surface by turning it to liquid water equivalent when it

reaches the surface (Vavrus 2007). More recently, studies have begun using prescribed, but realistic, boundary conditions to look at climate sensitivity within more physically reasonable bounds. These include studies of the effect of minimum/maximum sea ice extents (Alexander et al. 2004), historical and current land cover (Matthews et al. 2003; Brovkin et al. 2006), and realistic irrigation (Boucher et al. 2004).

We ran four simulations for 30 years with climatological sea surface temperatures and sea ice concentrations, and satellite observations of the seasonal cycle in vegetation. The first 10 years were discarded as spin up, and the latter 20 years used for comparison and statistical testing between simulations. In the CTRL case, the thermal conductivity of the snow was allowed to vary, as a function of equation (1). In SC-SOIL, the thermal conductivity of the snow was set to the thermal conductivity of the soil for each underlying grid cell, essentially removing any

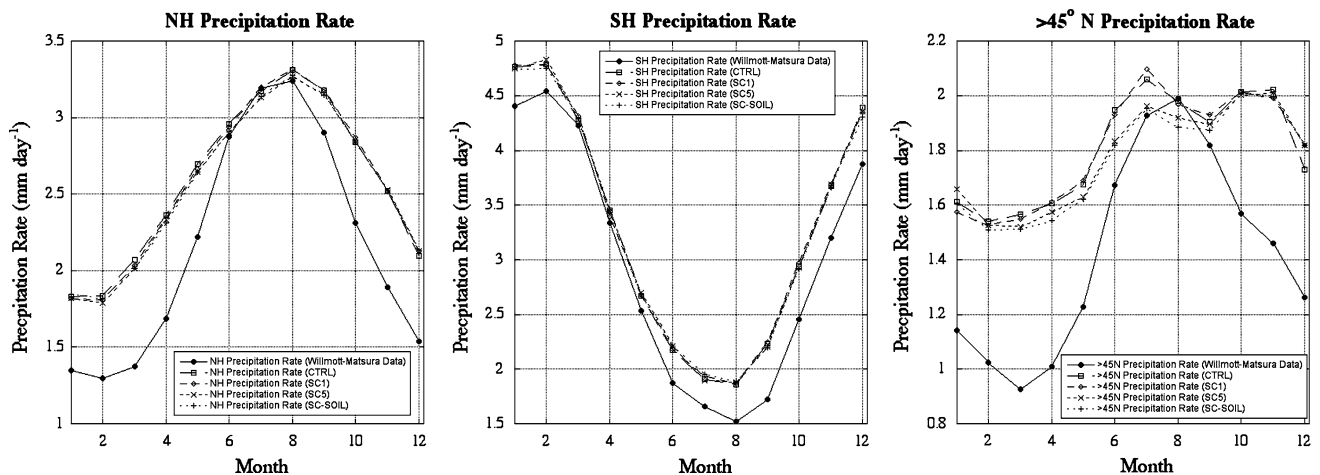


Fig. 6 As Fig. 4, but for precipitation rate (mm per day)

insulative effect. In SC-HI, the conductivity was set to $0.50 \text{ W m}^{-1} \text{ K}^{-1}$ (higher conductivity, decreasing the insulative effect), and in SC-LO it was set to $0.10 \text{ W m}^{-1} \text{ K}^{-1}$ (lower conductivity, increasing the insulative effect). For our analysis, we compare (using a two-sided Student's t test) SC-SOIL against CTRL and SC-HI against

SC-LO. The first comparison is our purely theoretical case, designed to address the maximum influence of the snow conductivity within the climate model. The second comparison, setting static thermal conductivities based on observed ranges, is intended to show the sensitivity of the model to a more realistic range of conductivities.

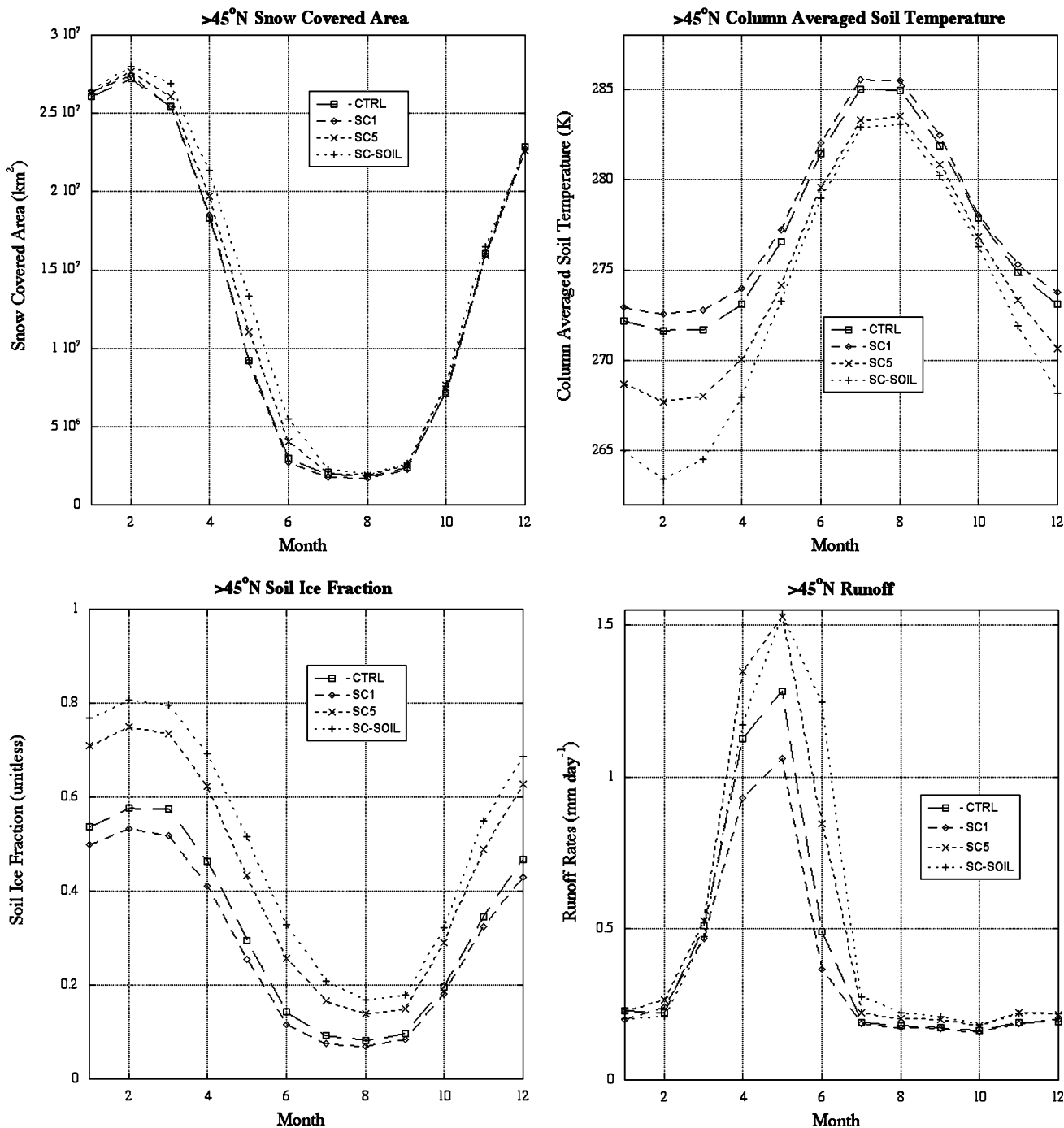


Fig. 7 A comparison between scenarios of the seasonal cycles in snow covered area, column averaged soil temperature, ground ice content, and runoff, for land areas north of 45° N

3 Results and discussion

All difference maps show seasonal or annual differences, with insignificant differences ($P > 0.05$) masked out, as determined by a two-sided Student's t test. Difference maps compare high conductivity/low insulation cases (SC-SOIL and SC-HI) against cases with lower conductivity/higher insulation (CTRL and SC-LO). The comparisons are SC-SOIL minus CTRL (our theoretical case) and SC-HI minus SC-LO (our case with observed high and low snow conductivity values). Our results and discussion are focused on land regions in the mid to high northern latitudes ($>45^\circ$ N), an area that experiences extensive snow cover during the boreal winter season and a pronounced seasonal cycle in snow covered area. Here we expect the insulative effect of the snow cover to be most important. To ensure that the model reaches an equilibrium state after 10 years, we look at trends in the soil temperatures north of 45° N (Table 1). There are significant ($P \leq 0.10$) negative soil temperature trends in SC-SOIL and SC-HI, and significant positive trends in SC-LO. These trends, however, are anchored by the first 10 years of simulation (our spin up period). In the latter 20 years, the trends essentially disappear and become insignificant. Since soil temperatures are likely the longest memory component within our simulations, we can be reasonably assured that the model has reached a new equilibrium and the last 20 years are

Table 1 Trends (based on a linear least squares regression) in column averaged soil temperatures above 45° N

Simulation	Years 1–30		Years 1–10		Years 10–30	
	Slope	P value	Slope	P value	Slope	P -value
CTRL	−0.001	0.701	−0.035	0.141	−0.002	0.768
SC-SOIL	−0.017	0.037	−0.149	0.009	−0.004	0.619
SC-HI	−0.015	0.067	−0.098	0.064	−0.007	0.545
SC-LO	0.009	0.018	0.055	0.007	0.003	0.596

Shown are the trends in units of K per year for the entire time period of simulation (years 1–30), the spin up period (years 1–10), and the scenario comparison period (years 10–30). Significant trends ($P \leq 0.10$) are highlighted in bold

valid for our scenario comparisons. We begin with a comparison of the seasonal cycles for a selected group of variables among our simulations, and then examine spatial differences and their significance.

3.1 Seasonal cycles

We compare area averaged climatological seasonal cycles of temperature and precipitation over land from our model runs against validation data from the dataset of Willmott

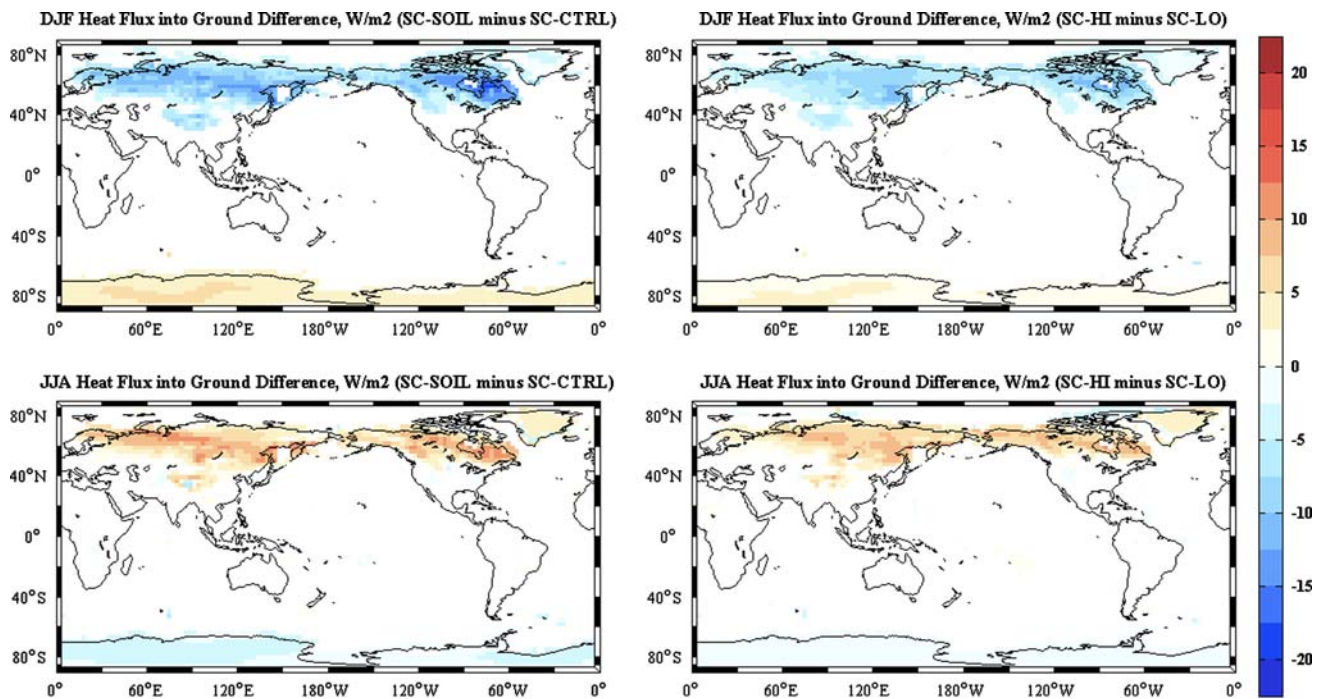


Fig. 8 Differences in heat flux into the ground (units of W m^{-2}) for SC-SOIL minus CTRL and SC-HI minus SC-LO. Positive values represent an anomalous heat flux from the atmosphere to the ground; negative values indicate and anomalous heat flux from the ground to

the atmosphere. Top row shows results from boreal winter (DJF) comparison, bottom row shows results from boreal summer (JJA) comparison

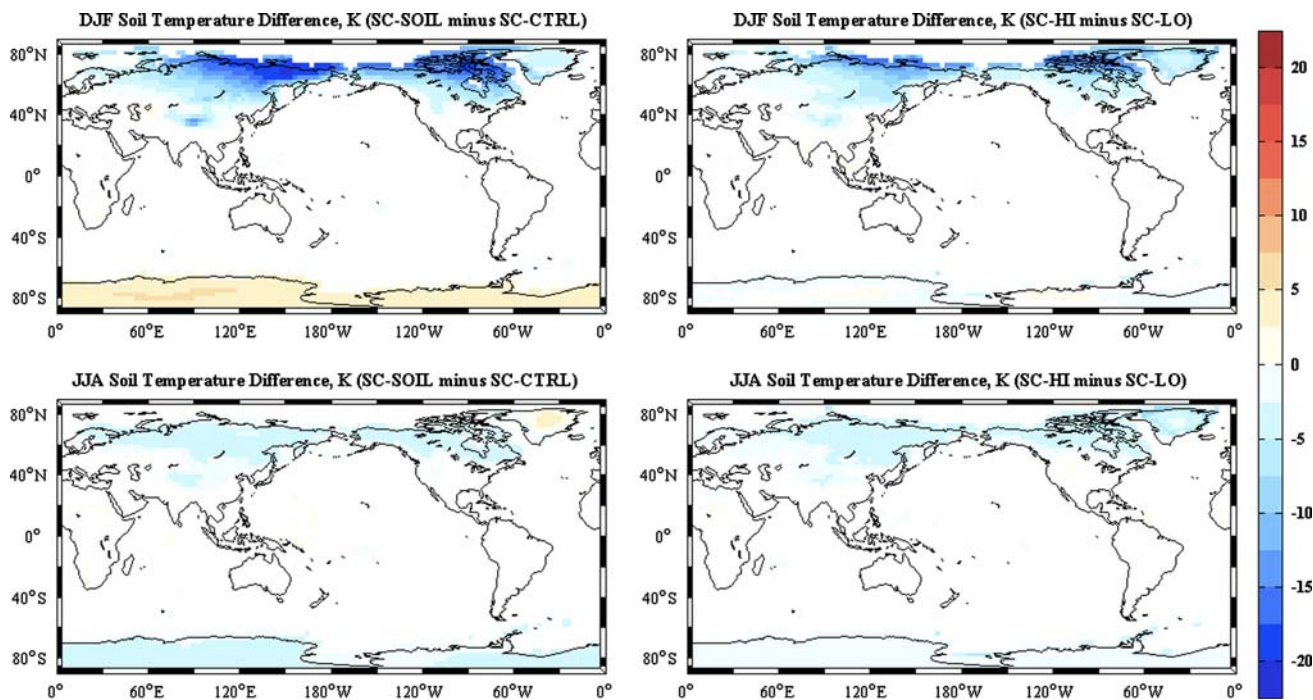


Fig. 9 Differences in mean soil column temperature ($^{\circ}\text{C}$) for SC-SOIL minus CTRL and SC-HI minus SC-LO, for seasons DJF and JJA. *Top row* shows results from boreal winter (DJF) comparison, *bottom row* shows results from boreal summer (JJA) comparison

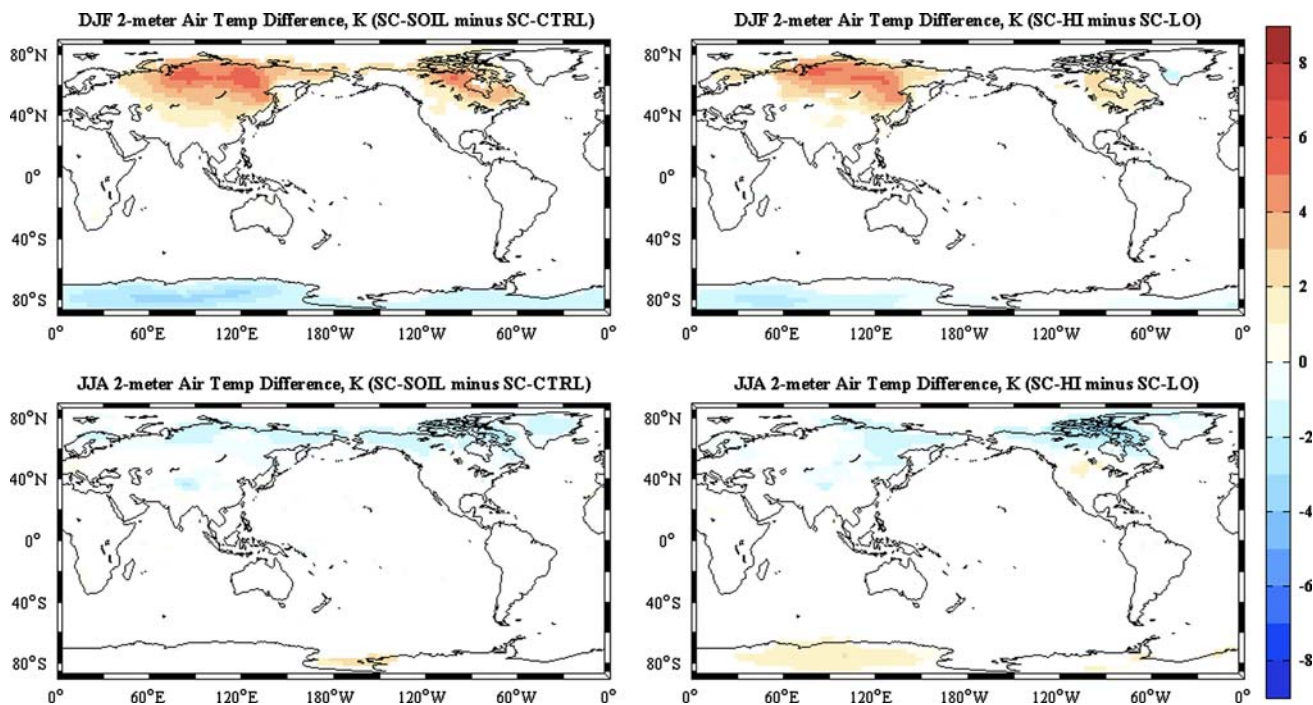
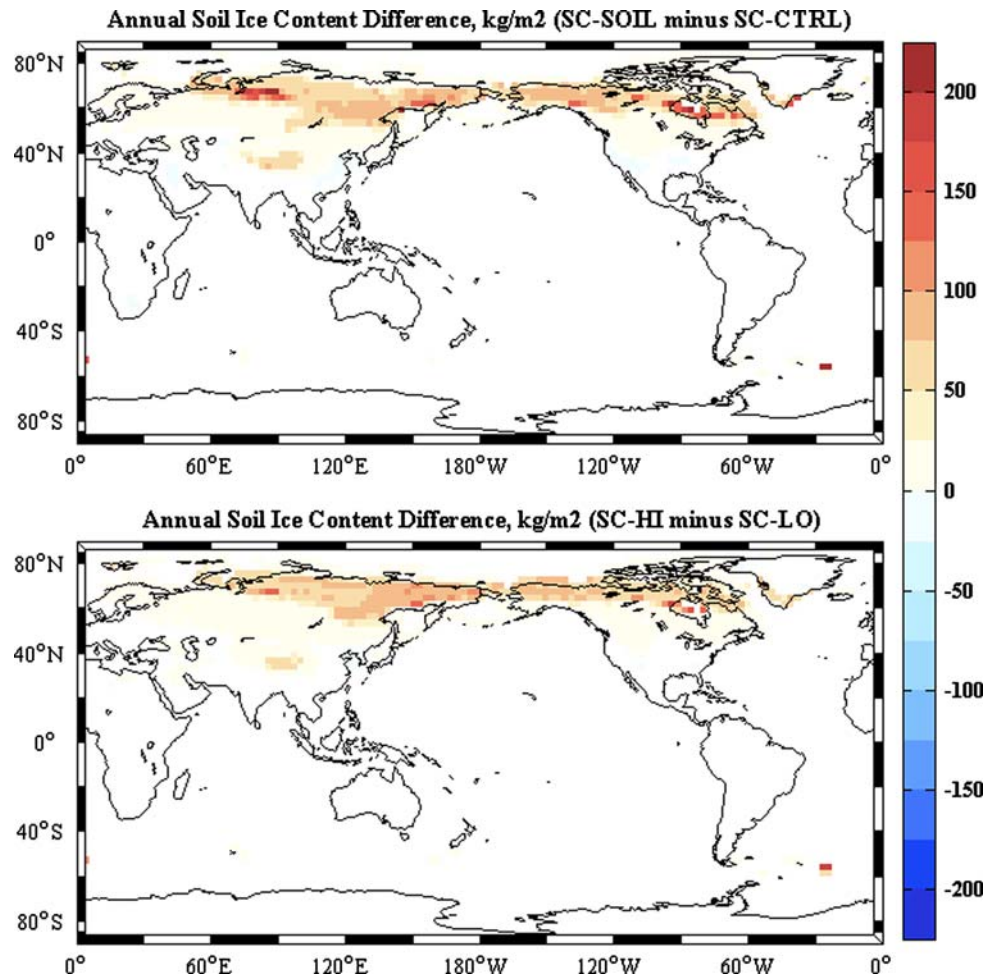


Fig. 10 Differences in 2-m air temperature ($^{\circ}\text{C}$) for SC-SOIL minus CTRL and SC-HI minus SC-LO, for seasons DJF and JJA. *Top row* shows results from boreal winter (DJF) comparison, *bottom row* shows results from boreal summer (JJA) comparison

Fig. 11 Annual differences in mean soil ice content (kg m^{-2}) for SC-SOIL minus CTRL and SC-HI minus SC-LO



and Matsuura (2000). We make this comparison for three regions separately: the Northern Hemisphere, the Southern Hemisphere, and land areas north of 45°N (our main region of interest).

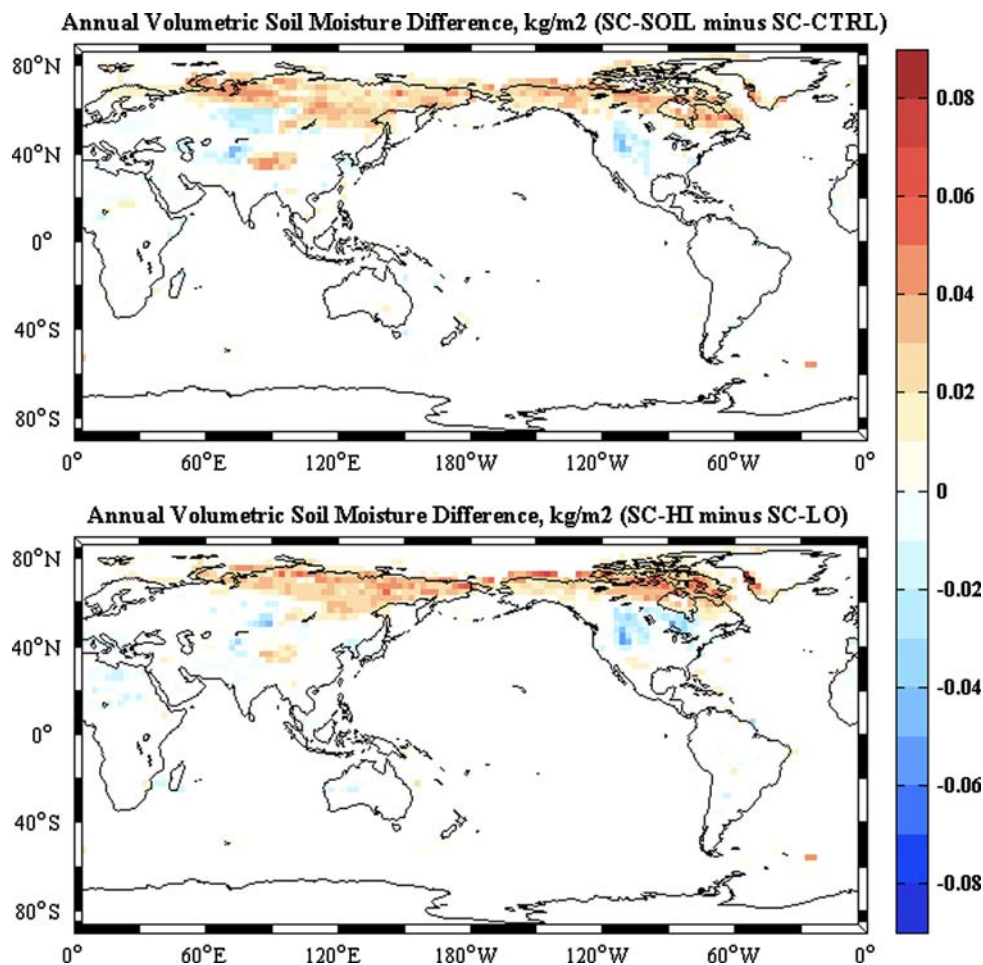
Results from our CTRL simulation compare favorably to results from previous validation studies (Dickinson et al. 2006). For temperature (Fig. 5), our CTRL simulation captures the seasonal cycle well in all three regions. A major discrepancy is the previously mentioned warm bias in the model, most pronounced during the winter seasons (DJF in the Northern Hemisphere, JJA in the Southern Hemisphere). Differences between the model scenarios are most clearly seen in the $>45^\circ\text{N}$ graph. Beginning in October, SC-HI and SC-SOIL air temperatures begin to show differences from SC-LO and CTRL. These differences increase through the early winter, with warmer temperatures in the high conductivity scenarios of about 1–3 K in December, showing the relatively higher importance of the thermoinsulative effect of snow cover during the fall and winter than the spring. Beginning in March, the sign of the scenario differences actually reverses, with the high conductivity scenarios showing slightly cooler near-

surface air temperatures. In this case, lower soil temperatures (discussed later) drive an increased heat flux from the atmosphere to the soil, cooling the near-surface air temperatures.

For precipitation, the model shows a clear wet bias with a dampened seasonal cycle, especially during the winter in the Northern Hemisphere (Fig. 6). Model run differences are clearest for spring and summer above 45°N ; here the low conductivity scenarios show higher precipitation rates than the high conductivity scenarios. This finding is most likely due to land surface hydrology changes in the high conductivity scenarios, which lead to reduced evapotranspiration and cloud cover (discussed later).

We also show seasonal cycles from our simulations for snow-covered area, column averaged soil temperature, soil ice, and runoff, north of 45°N (Fig. 7). Consistent with lower surface air temperatures, SC5 and SC-SOIL show a more extensive snow covered area in the spring and later winter. The simulations begin to diverge in February, and the differences increase through the spring, indicative of a delayed seasonal snowmelt from lower surface air temperatures in the high conductivity cases. Soil temperatures

Fig. 12 Annual differences in volumetric soil moisture content (mm^3 per mm^3) for SC-SOIL minus CTRL and SC-HI minus SC-LO

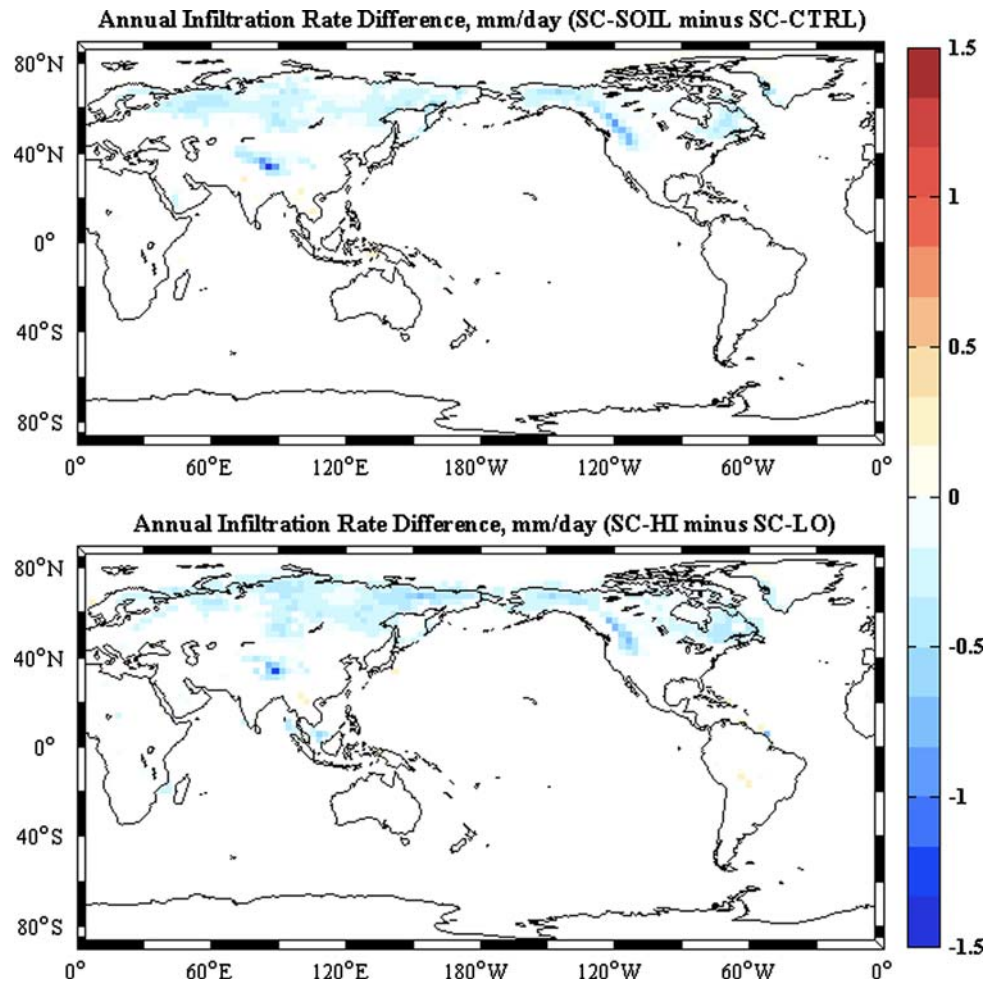


are also lower in these high conductivity simulations, with peak anomalies during the boreal winter (February and March) that become damped into the spring and summer. For the theoretical comparison (SC-SOIL minus CTRL), area averaged soil temperatures differences are -7 to -8 K; for the realistic comparison (SC5 minus SC1) the differences are about -4 to -5 K. Our static low conductivity scenario, SC1, shows slightly higher soil temperatures compared to CTRL ($+1$ K). Along with changes in soil temperatures, the simulations show pronounced differences in the proportion of soil moisture existing as ground ice, expressed relative to total soil moisture (solid and liquid). Increases (in SC1 and SC-SOIL) are as high as 20% during the winter months, compared to CTRL and SC1, and these anomalies persist through the year. By reducing soil permeability, increased ground ice also affects runoff. The timing of spring runoff remains the same, peaking in May and corresponding to the spring snowmelt, but the magnitudes differ sharply. Simulations with higher proportions of ground ice show higher runoff rates; the increases exist throughout the year, but are largest during the April–June period.

3.2 Soil and air temperatures

In both sets of comparisons (SC-SOIL minus CTRL and SC-HI minus SC-LO) there is an asymmetric seasonal response in the ground heat flux (Fig. 8). During the boreal winter period (DJF), heat flux anomalies in the boreal regions of the Northern Hemisphere are from the ground to the atmosphere, over areas that experience persistent snow cover over most of the winter: the snow pack first forms in the autumn or late summer, building in mass and extent until the spring melt. The snow acts as a persistent layer of insulation, retarding heat exchange between the soil and atmosphere and, as a result, winter soil temperatures can be much higher than the overlying atmosphere. By either removing or severely reducing the insulative effect (as in the SC-SOIL and SC-HI cases), heat exchange is increased, and anomalous heat flow is directed from the soils to the atmosphere. The winter heat loss from the soils is substantial enough to lead to much lower soil temperatures, with anomalies persisting throughout the year (Fig. 9). Column averaged soil temperatures are up to 20 K lower in some regions during the winter, and on the order of 5–6 K

Fig. 13 Annual differences in infiltration rate (mm per day) for SC-SOIL minus CTRL and SC-HI minus SC-LO



lower during the summer (JJA) season. The lower summer soil temperatures increase the temperature gradient between the soil and atmosphere. The increased temperature gradient explains the JJA heat flux anomalies from Fig. 8, where the anomalous heat flux is directed *into* the ground from the warmer atmosphere to the cooler soils. The alterations to the snow thermal conductivity, and subsequent changes in soil heat flux and soil temperatures, are enough to significantly influence near-surface air temperatures (Fig. 10). Anomalies are largest during the DJF period in the Northern Hemisphere, especially over Eurasia, where extensive, positive temperature anomalies reach 3–5 K. Temperature anomalies are reduced in magnitude and extent, and reversed in sign, for the JJA season, where negative anomalies of 1–2 K occur over roughly the same regions.

The seasonal response for all variables is generally of opposite sign in the Southern Hemisphere, confined predominantly over Antarctica, where snow persists year round. Anomalous ground heat fluxes during Austral summer (DJF) are directed from the atmosphere into the soil, during the Austral winter (JJA) they reverse and the

anomalous flux is from the soil to the atmosphere. Soil and air temperature anomalies are damped, relative to the Northern Hemisphere, but are still present and controlled by the same mechanisms that explain the patterns north of the equator.

3.3 Surface hydrology and photosynthesis

The extensive reduction in soil temperatures has a significant effect on soil hydrology. Annual average ground ice content (Fig. 11) increases, mirrored by roughly equal decreases in soil liquid water content (not shown). Total volumetric soil moisture content (both ice and liquid) changes as well (Fig. 12), showing some minor (but significant) increases over large regions of the Northern Hemisphere, as well as some areas of decreased moisture.

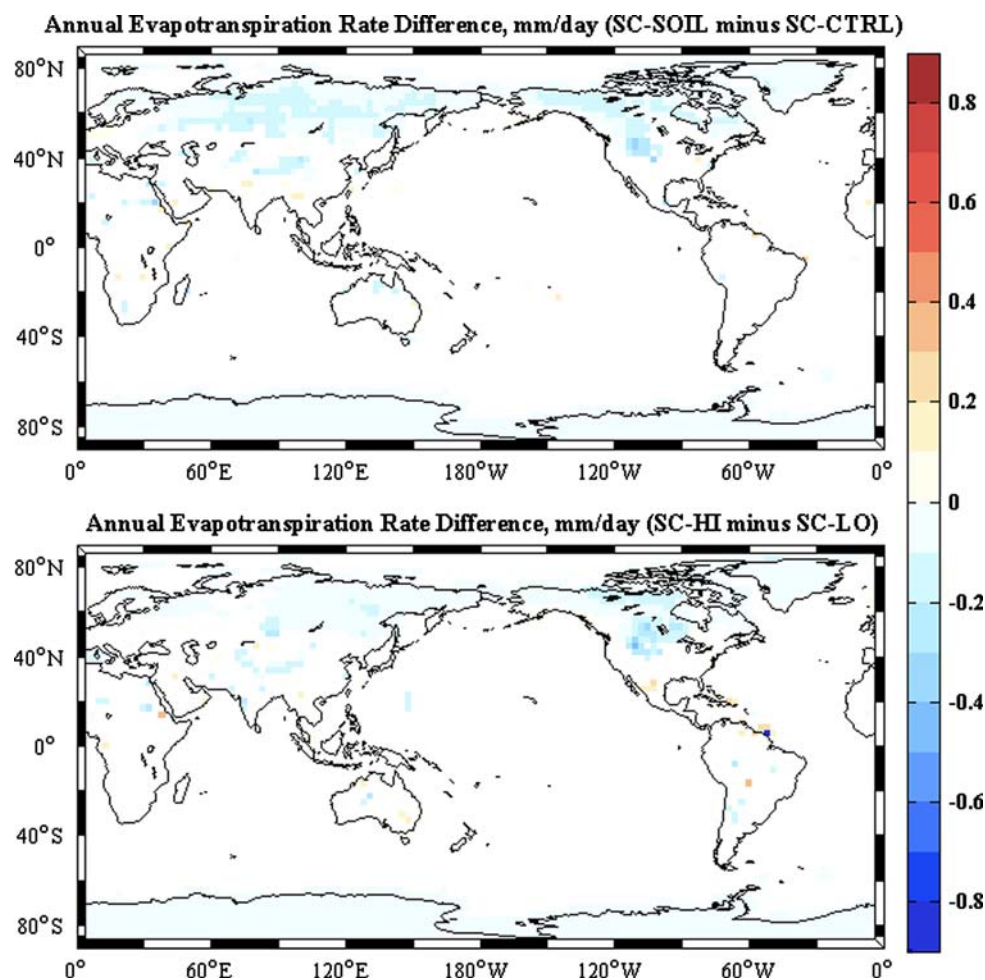
The total soil moisture changes are driven by several processes. As the ice content in the soil increases, pore spaces within the soil matrix become filled and infiltration of water into the soil decreases (Fig. 13). Surface water inputs that would normally recharge the soil instead get

Table 2 Selected surface variables, averaged over the Northern Hemisphere mid to high latitudes (45° N–90° N)

Area average (45° N–90° N) surface energy fluxes ($W\ m^{-2}$) DJF												
MAM												
Latitude 45°–90° Flux	CTRL	SC1	SC5	SC-NONE	Difference SC-SOIL-CTRL	Difference SC5-SC1	CTRL	SC1	SC5	SC-NONE	Difference SC-SOIL-CTRL	Difference SC5-SC1
Latitude 45°–90° Flux	CTRL	SC1	SC5	SC-NONE	Difference SC-SOIL-CTRL	Difference SC5-SC1	CTRL	SC1	SC5	SC-NONE	Difference SC-SOIL-CTRL	Difference SC5-SC1
Incident solar	28.61	28.87	28.21	28.12	-0.48	-0.66	212.40	210.81	213.52	216.71	4.31	2.71
Absorbed solar	17.30	17.35	17.06	16.97	-0.32	-0.29	125.28	124.27	123.62	122.65	-2.63	-0.65
Reflected solar	11.31	11.53	11.15	11.15	-0.16	-0.38	87.13	86.54	89.91	94.06	6.93	3.36
Heat flux into ground	-11.94	-9.95	-17.70	-22.04	-10.10	-7.75	4.02	4.15	5.49	9.92	5.90	1.34
SH flux	19.02	18.83	19.57	19.63	0.62	0.74	31.91	32.20	30.51	28.60	-3.31	-1.69
LH flux	8.42	7.91	10.03	10.85	2.43	2.12	24.86	24.60	24.47	23.25	-1.61	-0.13
Snow melt heat flux	1.27	1.26	1.17	0.97	-0.29	-0.09	8.27	7.93	8.55	8.33	0.06	0.61
JJA												
SON												
Latitude 45°–90° Flux	CTRL	SC1	SC5	SC-NONE	Difference SC-SOIL-CTRL	Difference SC5-SC1	CTRL	SC1	SC5	SC-NONE	Difference SC-SOIL-CTRL	Difference SC5-SC1
Latitude 45°–90° Flux	CTRL	SC1	SC5	SC-NONE	Difference SC-SOIL-CTRL	Difference SC5-SC1	CTRL	SC1	SC5	SC-NONE	Difference SC-SOIL-CTRL	Difference SC5-SC1
Incident solar	284.15	286.65	286.65	287.97	3.82	0.32	72.38	72.30	72.73	73.00	0.62	0.43
Absorbed solar	209.49	212.95	209.01	206.88	-2.61	-3.94	55.59	55.63	55.86	56.03	0.44	0.23
Reflected solar	74.66	73.71	77.96	81.08	6.42	4.25	16.79	16.68	16.88	16.97	0.18	0.20
Heat flux into ground	15.45	14.08	19.34	21.56	6.11	5.27	-13.21	-12.95	-15.26	-17.83	-4.61	-2.32
SH flux	56.76	57.97	53.71	52.10	-4.66	-4.26	32.44	32.19	32.30	32.30	-0.14	0.11
LH flux	35.51	36.04	35.53	34.44	-1.08	-0.51	12.92	12.78	13.27	13.62	0.70	0.49
Snow melt heat flux	3.62	3.34	5.46	6.34	2.72	2.11	0.90	0.89	0.86	0.79	-0.11	-0.03

Averaging is done by season; December through February (DJF), March through May (MAM), June through August (JJA), and September through November (SON)

Fig. 14 Annual differences in evapotranspiration rate (mm per day) for SC-SOIL minus CTRL and SC-HI minus SC-LO

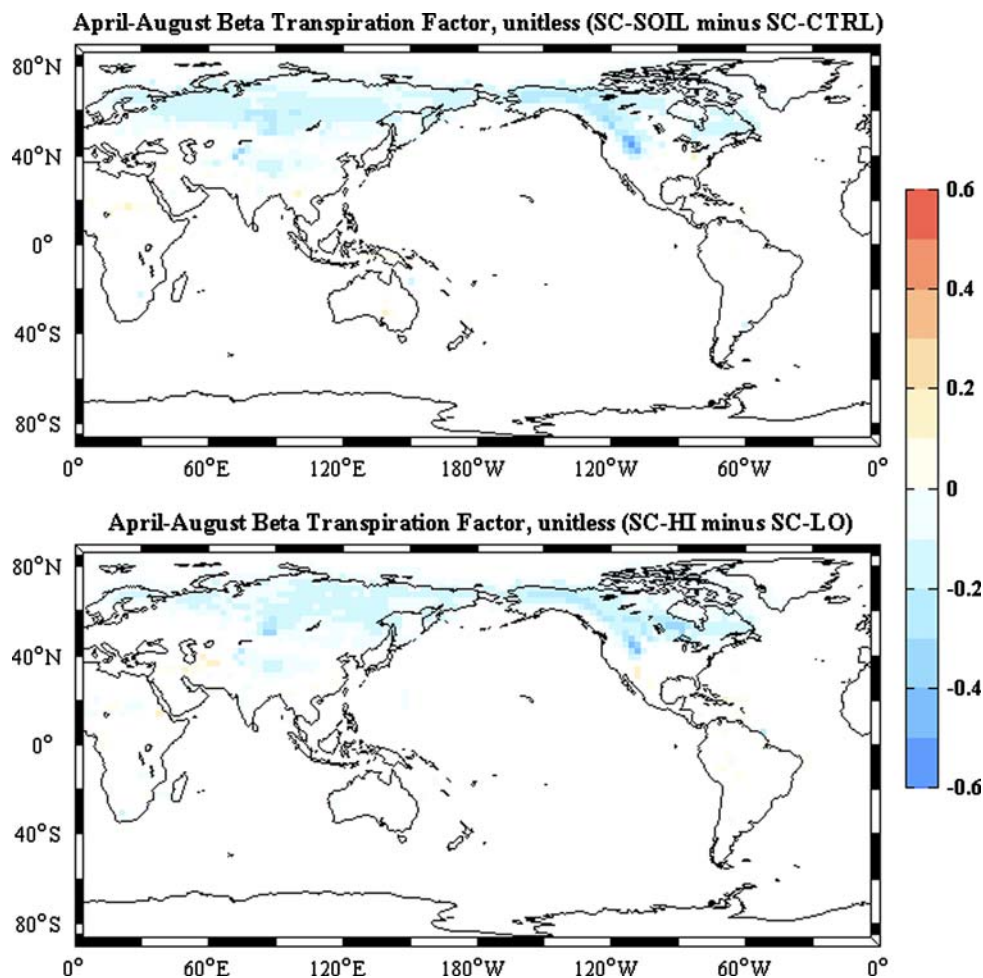


shifted to runoff, helping to explain regions where the soils are drier. Most areas, however, actually indicate wetter soils; over these same regions there are large reductions in evapotranspiration (Fig. 14), driven by two different factors. Physical evaporation decreases are largely a response to cooler air temperatures, reducing the evaporative demand of the atmosphere. Just as important, however, are changes in transpiration, the flux of water from the soil to the atmosphere through the plants.

Figure 15 shows the differences in the beta transpiration function for the April through August period, the period that encompasses all or most of the growing season (when transpiration is most active) in the Northern Hemisphere. The beta function represents soil moisture limitations on transpiration, the surface to atmosphere fluxes of water through the vegetation. Values for the function range from zero to unity, where zero completely shuts down transpiration and one indicates soil moisture does not limit transpiration. The beta function is a function of soil wetness (i.e., liquid moisture in the soil) and rooting depth (i.e., how much of the soil moisture the plant can access). The increases in ground ice in our experiments influence

the beta function (and, subsequently, transpiration) by modulating soil wetness: the soil wetness decreases as soil liquid water content declines or increased ground ice content hinders water uptake by roots. In our scenarios we saw little reduction (and, in fact, some increases) in total soil water (frozen and liquid). However, there was a significant shift from liquid soil water to soil ice with the colder soils. This led to large reductions in transpiration (via the beta function) that contributed to the overall decrease in evapotranspiration. Transpiration directly influences ecosystem functioning through photosynthesis. Within the model, the beta transpiration function directly impacts V_{\max} , the maximum rate of carboxylation, an important input into the photosynthesis calculation. Our high conductivity/low insulation experiments show widespread decreases in photosynthesis (Fig. 16). It is difficult to ascribe the reduction in photosynthesis directly to the reductions in transpiration from increased ground ice content, as soil and air temperatures may also be influencing photosynthesis. The change in the beta transpiration function, however, does suggest that hydrologic factors may be playing a role, in addition to temperature.

Fig. 15 April through August differences in beta transpiration factor (unitless) for SC-SOIL minus CTRL and SC-HI minus SC-LO



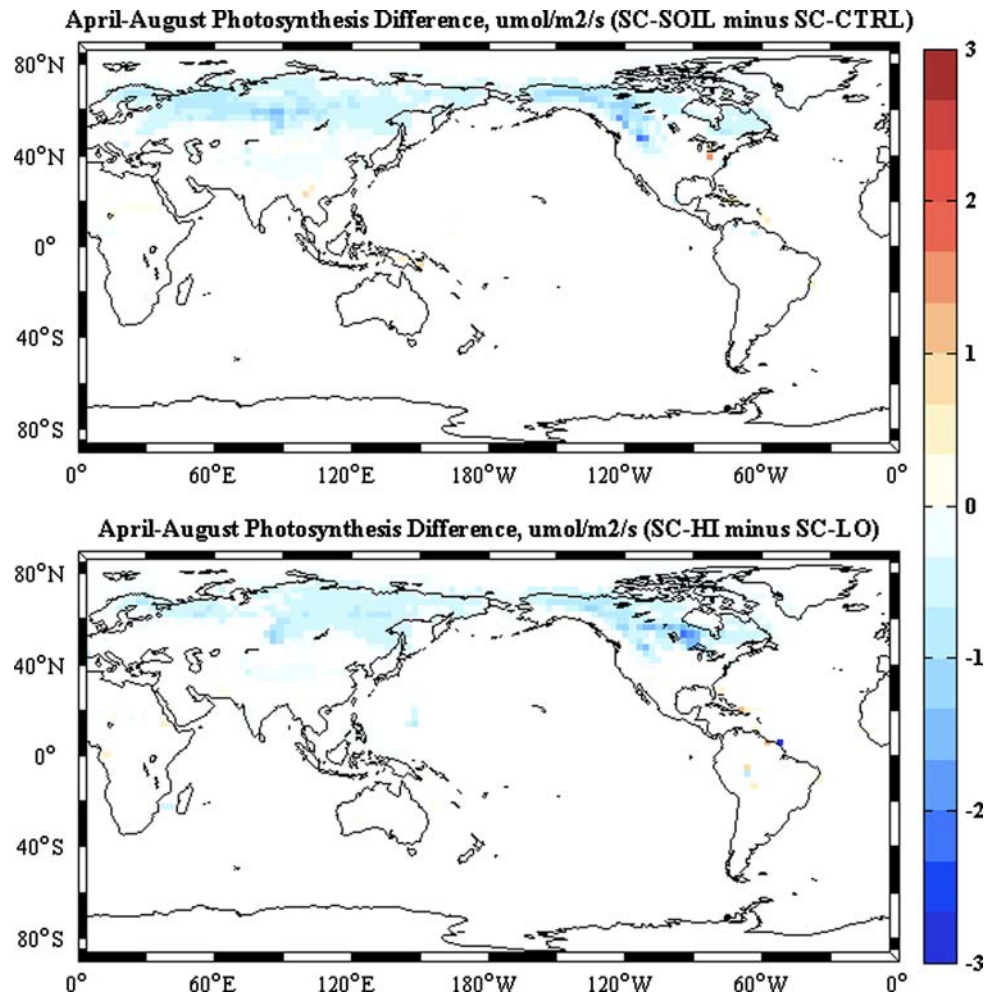
We present the changes in total soil moisture (Fig. 12) cautiously. In general, permafrost soils are close to saturation, as permafrost provides an impenetrable barrier to water movement (Lawrence and Slater 2005; Serreze et al. 2003). Permafrost soils (and most soils) in our CTRL simulation, however, are almost uniformly below saturation. As mentioned previously, this dry soil bias in CLM3 is reduced by hydrologic adjustments (Lawrence et al. 2007), but it is not eliminated, as some of the error comes from the atmosphere model, CAM3 (Dickinson et al. 2006). Therefore, some of the soil moisture increases in our model may reflect simply a reduction in the dry soil bias from reductions in evapotranspiration.

3.4 Surface energy balance

The first order effect of changing the snow thermal conductivity will be to modify the heat exchange between the soils and atmosphere. To confirm that the differences in our scenarios are driven primarily by this anomalous flux, we look at the high and mid-latitude (45° N– 90° N) surface

energy balance for the Northern Hemisphere, where most of the model response occurs (Table 2). During DJF and SON, changes in the surface energy balance are dominated almost entirely by changes in the ground heat flux, with anomalous heat fluxes directed from the ground to the atmosphere. There are some minor increases to the latent heat flux in DJF, but these are small and tend to be localized in areas with anomalously high soil moisture. In MAM and JJA ground heat flux anomalies are reduced somewhat in magnitude and switch signs, signifying an anomalous flux from the atmosphere into the soil. During these seasons, however, there also appear to be large anomalies in other components of the surface energy balance. The increase in incident solar radiation is driven by reductions in cloud cover, a consequence of reduced evapotranspiration and lower atmospheric moisture. The increase in reflected solar radiation and reduction in absorbed radiation are caused by increased albedo associated with increased snow cover during these seasons. Albedo increases reach 0.12 and 0.15 in MAM and JJA, respectively, associated with increases in fractional snow coverage of up to 0.40 in both seasons. The increased snow cover is partially a result of minor snowfall increases

Fig. 16 April through August differences in photosynthesis ($\mu\text{mol m}^{-2} \text{s}^{-1}$) for SC-SOIL minus CTRL and SC-HI minus SC-LO



in some areas, but is primarily a result of delayed snowmelt from lower near-surface air temperatures. The energy balance table highlights some of the seasonal characteristics of various snow feedback mechanisms. During fall and winter, anomalies associated with the thermoinsulation effect (i.e., the ground heat flux) dominate over the other anomalies. In the spring and early summer, however, anomalies associated with snow albedo feedbacks (i.e., reflected and absorbed radiation) reach similar magnitudes as the ground heat flux. These results suggest altered snow conductivity may also affect the soil and surface climate indirectly by, for example, altering snow cover and surface albedo.

4 Conclusions

We used a global general circulation model to test the sensitivity of land surface and climate processes to snow thermal conductivity. Our study differs from other climate modeling studies investigating snow in the climate system (e.g., Vavrus 2007) in that we examined the thermoinsulation effect independent of other snow properties. We found

some results consistent with other theoretical studies (e.g., Molders and Walsh 2004): higher snow thermal conductivity (scenarios SC-SOIL and SC-HI) led to significantly colder soils that remained cool (relative to CTRL and SC-LO) even into the summer/snow-free season. Soil temperatures cooled as much as 20 K in winter; these negative anomalies were reduced, but still carried over into the summer. The increased heat exchange was also enough to significantly influence near-surface air temperatures, leading to wintertime temperature increases of about +3 to +6 K. The colder soils, in turn, also drove increased heat flux into the ground during the summer, with resulting air temperature anomalies of -1 to -2 K. This is a result that has not been previously reported, showing the potential for changes in land-atmosphere heat exchange to influence near-surface climate. Somewhat surprisingly, the magnitude of model response was similar for both the theoretical (SC-SOIL minus CTRL) and realistic (SC-HI minus SC-LO) comparisons. This finding could be related to the fact that, in the Northern Hemisphere, CTRL thermal conductivity values are biased towards the low end of the observed range (Fig. 1). The model responses in hydrology,

photosynthesis, and snow cover suggest that temperature changes associated with altered conductivity can significantly alter other components of the land surface as well.

The thermoinsulative effect of snow can be altered by either changing the snow *quantity*, adding or removing snow, or *quality*, by altering snow density (e.g., Sokratov and Barry 2002; Zhang et al. 1996). Through melting and refreezing, compaction, and contact metamorphism, the conductivity of snow can change substantially over time. With warmer temperatures, snowpack can be substantially reduced or completely removed. If this occurs in the autumn, when the conductivity effects outweigh the albedo effects (Zhang 2005), this may act to counter surface warming induced by albedo related snow cover feedbacks (Groffman et al. 2001; Handy et al. 2001; Vavrus 2007). The work we present shows that, even over realistic bounds, changes in snow conductivity alone can be substantial enough to cause a significant response at the land surface and near-surface climate. This adds an additional level of uncertainty to various GCM projections of changes in permafrost (e.g., Anisimov and Nelson 1997; Anisimov et al. 1997; Goulden et al. 1998; Stendel and Christensen 2002; Lawrence and Slater 2005). If the models do not accurately capture either the quantity of snow (depth or cover) or quality of snow (the thermal conductivity) over time (either seasonally or interannually), this conductivity effect could lead to erroneous or diverging predictions. Results here also support other recent studies, showing the important role low thermal conductivity layers (such as snow or organic matter) have on permafrost dynamics and soil temperatures within global climate models (Alexeev et al. 2007; Lawrence and Slater 2007).

Acknowledgments This work was supported, in part, by NSF Grant #OPP-0531166, Greening of the Arctic. The authors wish to thank two anonymous reviewers for useful comments. BIC acknowledges the academic and financial support of the University of Virginia Department of Environmental Sciences and the National Center for Atmospheric Research. The National Center for Atmospheric Research is sponsored by the National Science Foundation.

References

- Alexander MA, Bhatt US, Walsh JE, Timlin MS, Miller JS, Scott JD (2004) The atmospheric response of realistic Arctic sea ice anomalies in an AGCM during winter. *J Clim* 17:890–905
- Alexeev VA, Ncolsky DJ, Romanovsky VE, Lawrence DM (2007) An evaluation of deep soil configurations in the CLM3 for improved representation of permafrost. *Geophys Res Lett*, 34. doi:10.1029/2007GL029536
- Anisimov OA, Nelson FE (1997) Permafrost zonation and climate change in the northern hemisphere: results from transient general circulation models. *Clim Change* 35:241–258
- Anisimov OA, Shiklamanov NI, Nelson FE (1997) Global warming and active-layer thickness: results from transient general circulation models. *Glob Planet Change* 15:61–77
- Armstrong RL, Brodzik MJ (2005) Northern hemisphere EASE-Grid weekly snow cover and sea ice extent version 3. National Snow and Ice Data Center, Boulder (Digital Media)
- Barnett TP, Dumenil L, Schlese U, Roeckner E, Latif M (1989) The effect of eurasian snow cover on regional and global climate variations. *J Atmos Sci* 46:661–686
- Barry RG, Armstrong R, Callaghan T et al (2007) Snow. In: *Global outlook for ice & snow*. United Nations Environment Programme, pp 39–62
- Bonan GB, Pollard D, Thompson SL (1992) Effects of boreal forest vegetation on global climate. *Nature* 359:716–718
- Bonan GB, Oleson KW, Vertenstein M, Levis S, Zeng X, Dai Y, Dickinson RE, Yang ZL (2002) The land surface climatology of the Community Land Model coupled to the NCAR Community Climate Model. *J Clim* 15:3123–3149
- Boucher O, Myhre G, Myhre A (2004) Direct human influence of irrigation on atmospheric water vapour and climate. *Clim Dyn* 22:597–603
- Boville BA, Rasch PJ, Hack JJ, McCaa JR (2006) Representation of clouds and precipitation processes in the community atmosphere model version 3 (CAM3). *J Clim* 19:2184–2198
- Brovkin V, Claussen M, Driesschaert E, Fichefet T, Kicklighter D, Loutre MF, Matthews HD, Ramankutty N, Schaeffer M, Sokolov A (2006) Biogeophysical effects of historical land cover changes simulated by six Earth system models of intermediate complexity. *Clim Dyn* 26:587–600
- Brown RD (2000) Northern hemisphere snow cover variability and change, 1915–97. *J Clim* 13:2339–2355
- Cary JW, Campbell GS, Papendick RI (1978) Is the soil frozen? An algorithm using weather records. *Water Resour Res* 14:1117–1122
- Cess RD, Potter GL, Zhang MH (1991) Interpretation of snow-climate feedback as produced by 17 general circulation models. *Science* 253:888–892
- Chapin FS, Shaver GR, Giblin AE, Nadelhoffer KJ, Laundre JA (1995) Responses of Arctic Tundra to experimental and observed changes in climate. *Ecology* 76:694–711
- Cohen J, Rind D (1991) The effect of snow cover on the climate. *J Clim* 4:689–706
- Cohen J, Entekhabi D (1999) Eurasian snow cover variability and northern hemisphere climate predictability. *Geophys Res Lett* 26:345–348
- Collins WD, Rasch PJ, Boville BA, Hack JJ, McCaa JR, Williamson DL, Kiehl JT, Briegleb B, Bitz C, Lin SJ, Zhang M, Dai Y (2004) Description of the NCAR community atmosphere model (CAM3). Technical Note NCAR/TN-464 + 5TR, National Center for Atmospheric Research, P.O. Box 3000, Boulder, Colorado, 80307-3000, 226 p
- Collins WD, Bitz CM, Blackmon ML, Bonan GB, Bretherton CS, Carton JA, Change P, Doney SC, Hack JJ, Henderson TB, Kiehl JT, Large WG, McKenna DS, Santer BD, Smith RD (2006a) The community climate system model version 3 (CCSM3). *J Clim* 19:2122–2143
- Collins WD, Rasch PJ, Boville BA, Hack JJ, McCaa JR, Williamson DL, Briegleb BP, Bitz CM, Lin SJ, Zhang M (2006b) The formulation and atmospheric simulation of the Community Atmosphere Model: CAM3. *J Clim* 19:2144–2161
- Dickinson RE, Oleson KW, Bonan GB, Hoffman F, Thornton PE, Vertenstein M, Yang ZL, Zeng X (2006) The Community Land Model and its climate statistics as a component of the Community Climate System Model. *J Clim* 19:2302–2324
- Farouki OT (1981) The thermal properties of soils in cold regions. *Cold Reg Sci Technol* 5:67–75
- Frei A, Gong G (2005) Decadal to century scale trends in North American snow extent in coupled atmosphere–ocean general circulation models. *Geophys Res Lett* 32. doi:10.1029/2005GL023394

- Gallimore R, Jacob R, Kutzbach J (2005) Coupled atmosphere–ocean–vegetation simulations for modern and mid-Holocene climates: role of extratropical vegetation cover feedbacks. *Clim Dyn* 25:755–776
- Goodrich LE (1982) The influence of snow cover on the ground thermal regime. *Can Geotech J* 19:421–432
- Goulden ML, Wofsy SC, Harden JW et al (1998) Sensitivity of boreal carbon balance to soil thaw. *Science* 279:214–217
- Groffman PM, Driscoll CT, Fahey TJ, Handy JP, Fitzhugh RD, Tiernay GL (2001) Colder soils in a warmer world: a snow manipulation study in a northern hardwood forest ecosystem. *Biogeochemistry* 56:135–150
- Handy JP, Groffman PM, Fitzhugh RD, Henry KS, Welman AT, Demers JD, Fahey TJ, Driscoll CT, Tiernay G, Nolan S (2001) Snow depth manipulation and its influence on soil frost and water dynamics in a northern hardwood forest. *Biogeochemistry* 56:151–174
- Hurrell JW, Hack JJ, Phillip AS, Caron J, Yin J (2006) The dynamical simulation of the community atmosphere model version 3 (CAM3). *J Clim* 19:2162–2183
- Jordan R (1991) A one-dimensional temperature model for a snow cover: technical documentation for SNTHERM, 89. U.S. Army Cold Regions Research and Engineering Laboratory, Special Report 91–16
- Kleidon A, Fraedrich K, Heimann M (2000) A green planet versus a desert world: estimating the maximum effect of vegetation on the land surface climate. *Clim Change* 44:471–493
- Hack JJ, Caron JM, Yeager SG, Oleson KW, Holland MM, Truesdale JE, Rasch PJ (2006) Simulation of the global hydrological cycle in the CCSM community atmosphere model version 3 (CAM3): mean features. *J Clim* 19:2199–2221
- Hall A (2004) The role of surface albedo feedback in climate. *J Clim* 17:1550–1568
- Hall A, Qiu X (2006) Using the seasonal cycle to constrain snow albedo feedback in future climate change. *Geophys Res Lett* 33. doi:10.1029/2005GL025127
- Hinzman LD, Kane DL, Bensen CS, Everett KR (1996) Energy balance and hydrological processes in an Arctic watershed. *Ecol Stud* 120:131–154
- Kane DL, Hinzman LD, Bensen CS, Liston GE (1991) Snow hydrology of a headwater Arctic basin. *Water Resour Res* 27:1099–1109
- Lawrence DM, Chase TN (2007) Representing a new MODIS consistent land surface in the Community Land Model (CLM 3.0). *J Geophys Res* 112. doi:10.1029/2006JG000168
- Lawrence DM, Slater AG (2005) A projection of severe near-surface permafrost degradation during the 21st century. *Geophys Res Lett* 32. doi:10.1029/2005GL025080
- Lawrence DM, Thornton PE, Oleson KW, Bonan GB (2007) The partitioning of evapotranspiration into transpiration, soil evaporation, and canopy evaporation in a GCM: impacts on land–atmosphere interaction. *J Hydrometeorol* 8:862–880
- Ling F, Zhang T (2003) Impact of the timing and duration of seasonal snow cover on the active layer and permafrost in the Alaskan Arctic. *Permafrost Periglacial Process* 14:141–150
- Luo L, Robock A, Vinnikov KY, Schlosser CA, Slater AG, Boone A, Braden H, Cox P, De Rosnay P, Dickinson RE, Dai Y, Duan Q, Etchevers P, Henderson-Sellers A, Gedney N, Gusev YM, Habets F, Kim J, Kowalczyk E, Mitchell K, Nasonova ON, Noilhan J, Pitman AJ, Schaake J, Shmakin AB, Smirnova TG, Wetzel P, Xue Y, Yang ZL, Zeng QC (2003) Effects of frozen soil on soil temperature, spring infiltration, and runoff: results from the PILPS 2(d) experiment at Valdai, Russia. *J Hydrometeorol* 4:334–351
- Matthews HD, Weaver AJ, Eby M, Meissner KJ (2003) Radiative forcing of climate by historical land cover change. *Geophys Res Lett* 30. doi:10.1029/2002GL016098
- Molders N, Walsh JE (2004) Atmospheric response to soil–frost and snow in Alaska in March. *Theor Appl Climatol* 77:77–105
- Nicolson DJ, Romanovsky VE, Alexeev VA, Lawrence DM (2007) Improved modeling of permafrost dynamics in a GCM land-surface scheme. *Geophys Res Lett*. doi:10.1029/2007GL029525
- Niu GY, Yang ZL (2006) Effects of frozen soil on snowmelt runoff and soil water storage at a continental scale. *J Hydrometeorol* 7:937–952
- Oleson KW, Dai Y, Bonan GB, Bosilovich M, Dickinson R, Dirmeyer P, Hoffman F, Houser P, Levis S, Niu GY, Thornton PE, Vertenstein M, Yang ZL, Zeng X (2004) Technical description of the community land model (CLM). Technical Note NCAR/TN-461 + STR, National Center for Atmospheric Research, P.O. Box 3000, Boulder, Colorado, 80307-3000, 173 p
- Qu X, Hall A (2006) Assessing snow albedo feedbacks in simulated climate change. *J Clim* 19:2617–2630
- Randall DA, Cess RD, Blanchet JP et al (1994) Analysis of snow feedbacks in 14 general circulation models. *J Geophys Res* 99:20,757–20772
- Sazonova TS, Romanovsky VE (2003) A model for regional-scale estimation of temporal and spatial variability of active layer thickness and mean annual ground temperatures. *Permafrost Periglacial Process* 14:125–139
- Serreze MC, Bromwich DH, Clark MP, Etringer AJ, Zhang T, Lammers R (2003) Large-scale hydro-climatology of the terrestrial Arctic drainage system. *J Geophys Res* 108. doi:10.1029/2001JD000919
- Shiklomanov NI, Nelson FE (1999) Analytic representation of the active layer thickness field, Kuparuk River Basin, Alaska. *Ecol Model* 123:105–125
- Shukla J, Mintz (1982) Influence of land–surface evapotranspiration on earth’s climate. *Science* 215:1498–1501
- Sokratov SA, Barry RG (2002) Intraseasonal variation in the thermoinsulation effect of snow cover on soil temperatures and energy balance. *J Geophys Res*. doi:10.1029/2001JD000489
- Stendel M, Christensen JH (2002) Impact of global warming on permafrost condition in a coupled GCM. *Geophys Res Lett* 29(13):10-1–10-4
- Sturm M, Racine C, Tape K (2001) Climate change: increasing shrub abundance in the Arctic. *Nature* 411:546–547
- Sturm M, Schimel J, Michaelson G, Welker JM, Oberbauer SF, Liston GE, Fahnestock J, Romanovsky VE (2005) Winter biological processes could help convert Arctic Tundra to Shrubland. *Bioscience* 55:17–26
- Vavrus S (2007) The role of terrestrial snow cover in the climate system. *Clim Dyn* 29:73–88
- Willis WO, Carlson CW, Alessi J, Hass HJ (1961) Depth of freezing and spring runoff as related to fall soil-moisture level. *Soil Sci Soc Am J* 41:115–123
- Willmott CJ, Matsuura K (2000) Terrestrial air temperature and precipitation. *Monthly and Annual Climatologies*. (Available online at <http://climate.geog.udel.edu/~climate>)
- Zhang T, Osterkamp TE, Stamnes K (1996) Influence of the depth hoar layer of the seasonal snow cover on the ground thermal regime. *Water Resour Res* 32:2075–2086
- Zhang T, Osterkamp TE, Stamnes K (1997) Effects of climate on the active layer and permafrost on the North Slope of Alaska, USA. *Permafrost Periglacial Process* 8:45–67
- Zhang T, Stamnes K, Bowling SA (2001) Impact of the atmospheric thickness on the atmospheric downwelling longwave radiation and snowmelt under clear-sky conditions in the Arctic and Subarctic. *J Clim* 14:920–939
- Zhang T (2005) Influence of the seasonal snow cover on the ground thermal regime: an overview. *Rev Geophys* 43. doi:10.1029/2005RG4002